

A Possible X-ray and Radio Counterpart of the High-Energy Gamma-ray Source 3EG J2227+6122

J. P. Halpern¹, E. V. Gotthelf, K. M. Leighly, and D. J. Helfand

Columbia Astrophysics Laboratory, Columbia University, 550 West 120th Street, New York, NY 10027

ABSTRACT

The identity of the persistent EGRET sources in the Galactic plane is largely a mystery. For one of these, 3EG J2227+6122, our complete census of X-ray and radio sources in its error circle reveals a remarkable superposition of an incomplete radio shell with a flat radio spectrum, and a compact, power-law X-ray source with photon index $\Gamma = 1.5$ and with no obvious optical counterpart. The radio shell is polarized at a level of $\simeq 25\%$. The anomalous properties of the radio source prevent us from deriving a completely satisfactory theory as to its nature. Nevertheless, using data from *ROSAT*, *ASCA*, the VLA, and optical imaging and spectroscopy, we argue that the X-ray source may be a young pulsar with an associated wind-blown bubble or bow shock nebula, and an example of the class of radio-quiet pulsars which are hypothesized to comprise the majority of EGRET sources in the Galaxy. The distance to this source can be estimated from its X-ray absorption as 3 kpc. At this distance, the X-ray and γ -ray luminosities would be $\approx 1.7 \times 10^{33}$ and $\approx 3.7 \times 10^{35}$ erg s⁻¹, respectively, which would require an energetic pulsar to power them.

If, on the contrary, this X-ray source is *not* the counterpart of 3EG J2227+6122, then by process of elimination the X-ray luminosity of the latter must be less than 10^{-4} of its γ -ray luminosity, a condition not satisfied by any established class of γ -ray source counterpart. This would require the existence of at least a quantitatively new type of EGRET source, as has been suggested in studies of other EGRET fields.

Subject headings: gamma rays: individual (3EG J2227+6122) — pulsars: general — supernova remnants — X-rays: observations

¹Visiting Astronomer, Kitt Peak National Observatory, National Optical Astronomy Observatories, which is operated by the Association of Universities for Research in Astronomy, Inc. (AURA) under cooperative agreement with the National Science Foundation.

1. Introduction

The nature of the persistent high-energy (> 100 MeV) γ -ray sources in the Galaxy remains an enigma almost three decades after their discovery. The third installment of the EGRET catalog (Hartman et al. 1999) lists a total of 270 sources, of which 93 are likely or possibly identified with blazars, five with rotation-powered pulsars, one with Cen A, and one with the LMC. This leaves 170 unidentified sources, of which 57, or one third, lie within $|b| \leq 10^\circ$ along the Galactic plane. This excess of low-latitude sources must comprise a Galactic population that is either similar to the already identified γ -ray pulsars, or representative of an entirely new class of γ -ray emitter associated with the disk population. These Galactic sources have proven extremely difficult to identify.

Rotation-powered pulsars are likely to dominate the Galactic γ -ray source population, but their detectability at both radio and γ -ray wavelengths depends on their beam patterns. The shapes of radio pulsar beams as determined by the rotating vector model (Radhakrishnan & Cooke 1969) demands that $\sim 50 - 70\%$ of young radio pulsars are *not* visible from Earth (Frail & Moffett 1993; Tauris & Manchester 1998). The clear differences between the broad observed γ -ray beam patterns and the narrow radio pulses implies that γ -ray emission is probably visible from a more complete range of directions than are the radio beams. Indeed, the identification of the high-energy γ -ray source Geminga as the first radio quiet, but otherwise ordinary pulsar (Halpern & Holt 1992; Bertsch et al. 1992), provides a likely prototype for the remaining unidentified Galactic sources. That Geminga was the brightest unidentified EGRET source, at a distance of only ~ 250 pc, argues that there should be others. The possible existence of intrinsically radio-quiet γ -ray pulsars also cannot be ruled out.

Several authors have considered the pulsar hypothesis from statistical or theoretical points of view (Halpern & Ruderman 1993; Helfand 1994; Kaaret & Cottam 1996). The most detailed theoretical treatment of the pulsar model for the Galactic γ -ray sources is that of Romani & Yadigaroglu (1995) and Yadigaroglu & Romani (1995;1997). They developed a numerical calculation of γ -ray production and beaming in the outer-gap model that successfully reproduces the basic observed features of the pulse profiles and the γ -ray efficiency as a function of age. By combining this model with a Monte Carlo simulation of the Galactic pulsar population, they estimated that a total of 22 pulsars should be detected by EGRET at the threshold of the first EGRET catalog. This number is very close to the actual number of unidentified sources at $|b| < 10^\circ$ in that catalog.

Candidate neutron-star identifications for additional EGRET sources have been found in the form of point-like X-ray sources with no obvious optical counterparts. One such candidate is present in the supernova remnant CTA1 which is close to 3EG J0010+7309 (Lamb & Macomb 1997; Brazier et al. 1998). Another one is in the γ -Cygni supernova remnant which is coincident with 3EG J2020+4017 (Brazier et al. 1996). Both of these so far lack detected pulsations. Most notable among the probable identifications is the radio star and Be/X-ray binary LSI +61°303

(Strickman et al. 1998) which has long been associated with the γ -ray source 2CG 135+01. Another possible candidate is a 34 ms X-ray pulsar with a Be star companion in the error circle of 3EG J0634+0521 (Kaaret et al. 1999; Cusumano et al. 2000). Additional EGRET sources have recently been tentatively identified with known radio pulsars based on the detection of a corresponding pulsed γ -ray signal, namely 3EG J1048–5840 with PSR B1046–58 (Kaspi et al. 2000), and the millisecond pulsar PSR J0218+4232 with 3EG J0222+4253 (Kuiper et al. 2000). X-ray synchrotron nebulae that are inferred to be powered by pulsars have been detected in the error circles of the EGRET sources 2EG J1811–2339 (Oka et al. 1999) and 3EG J1420–6038 (Roberts & Romani 1998; Roberts et al. 1999). PSR B1951+32 in the supernova remnant CTB 80 has been detected by EGRET (Ramanamurthy et al. 1995) even though it does not exceed the threshold for inclusion in the EGRET catalogs. It has also been suggested that accreting neutron-star binaries might be EGRET sources, although so far only one example has been found in the possible detection of intermittent γ -rays from Cen X-3 (Vestrand, Sreekumar, & Mori 1997).

Informed by the pulsar scenario, we are studying several EGRET sources that are at “intermediate” Galactic latitudes, $3^\circ < |b| < 8^\circ$, and that are not apparently variable. This strategy increases the likelihood that (a) the EGRET source is real, (b) its position is not affected by errors in the diffuse emission model or neighboring weak sources, (c) it is relatively nearby, (d) the intervening column density is not too large for soft X-ray observations, and (e) the corresponding optical fields are not too crowded. The absence of variability is important, since the known γ -ray pulsars show little if any long-term variability, while the blazars often flare dramatically.

One of our targets is 3EG J2227+6122, a source at Galactic coordinates $(\ell, b) = (106.^\circ 5, 3.^\circ 2)$ with a 95% error circle of radius $0.^\circ 46$ (Hartman et al. 1999). Its average flux is 4.1×10^{-7} photon $\text{cm}^{-2} \text{s}^{-1}$ (> 100 MeV) and its photon spectral index is 2.24 ± 0.14 . It is not obviously variable (McLaughlin et al. 1996). The total Galactic 21 cm column density in this direction is $8.2 \times 10^{21} \text{ cm}^{-2}$ (Stark et al. 1992). Prior to this work, there were no known pulsars or blazar-like radio sources in this field, and no prominent X-ray sources. In this paper we present the results of X-ray, radio, and optical observations of the region of 3EG J2227+6122 which together point to a possible identification.

2. Observations

2.1. ROSAT HRI Survey

The *ROSAT* HRI was used to cover the 95% error circle of 3EG J2227+6122 in four overlapping pointings, as shown in Figure 1. These observations were made during 1996 August 7–13. Exposure times ranged between 14,000 and 19,000 s. A total of six compact X-ray sources were detected in this field to a limiting count rate of approximately 1×10^{-3} counts s^{-1} . This limit corresponds to an intrinsic flux of 4×10^{-14} erg $\text{cm}^{-2} \text{s}^{-1}$ for a thermal plasma of $T = 3 \times 10^6$ K

and $N_{\text{H}} = 2 \times 10^{20} \text{ cm}^{-2}$, spectral parameters that are expected of stellar coronal X-ray sources which should be the dominant population in this field. The X-ray source positions, count rates, and optical counterpart data are listed in Table 1. Optical magnitudes and positions are taken from the USNO–A2.0 catalog (Monet et al. 1996).

2.2. Optical Identifications of *ROSAT* Sources

Optical spectroscopic identifications were made for five of the six *ROSAT* HRI sources using the KPNO 2.1m telescope and Goldcam spectrograph. Four of these sources are bright K and M type stars. The fifth is a bright emission-line star which is classified as a Herbig Ae/Be type by Hang, Liu, & Xia (1999); it is also an *IRAS* source. Our optical spectrum of this star is essentially identical to that of Hang et al., and it confirms their classification in detail. This star also illuminates a prominent nebulosity which is visible on the Palomar Observatory Sky Survey (POSS) plates. Our spectroscopy and subsequent $\text{H}\alpha$ imaging show that this nebula is bright in $\text{H}\alpha$. Herbig Ae/Be stars are commonly detected as X-ray sources (e.g., Zinnecker & Preibisch 1994), but we have no reason to suspect that this one is the origin of 3EG J2227+6122. We also note that the X-ray positions of all five identified sources are coincident with their optical positions to the expected statistical accuracy of $1'' - 3''$ (see Figure 2). Furthermore, any systematic offset between the average X-ray and optical positions is $\leq 0.''6$, which is not significantly different from zero. Therefore, we do not find it necessary to make any *a posteriori* adjustments to the X-ray astrometry.

The sixth HRI source, RX J2229.0+6114, remains unidentified optically. The remainder of this paper is largely concerned with the properties of this source and the evaluation of its credentials as a possible identification of 3EG J2227+6122. Within a conservative $5''$ error radius, which is justified empirically by the data in Figure 2, there is nothing at this location on the POSS plates. Figure 3 shows images of this field to a limit of $R = 24.5$ and $B = 24.0$ that we obtained using the MDM 2.4m telescope. The nearest bright object is a star of $R \approx 16.8$ which lies $5.''6$ southeast of the X-ray position; it is labeled star A in Figure 3. An optical spectrum which we obtained on the KPNO 2.1m telescope shows that it is in fact a highly reddened A star, an unlikely counterpart considering the hard X-ray properties of this source discussed below. The brightest object in the X-ray error circle, just north of star A, has $R = 21.3$. A Keck spectrum of this object kindly obtained by R. H. Becker shows no emission lines or other interesting features. Although we cannot firmly classify the spectrum, it is possibly an ordinary star or galaxy. On the other hand, if it is a truly featureless spectrum, then it could be a Crab-like pulsar or a BL Lac object. Nonetheless, we regard this X-ray source as unidentified to a limit of $R \geq 21.3$ and $B > 24$, and possibly to $R \geq 23$ if the $R = 21.3$ object is not its counterpart.

2.3. Radio Observations

We created a 20 cm image of the entire EGRET error circle for 3EG J2227+6122 by constructing a mosaic from 13 snapshots obtained on 31 March 1996 using the Very Large Array (VLA²) in its C configuration. The synthesized beam yields a resolution of $\approx 15''$ FWHM; the median rms in the image is 0.12 mJy. Subsequently, the NRAO/VLA Sky Survey (NVSS – Condon et al. 1998) covered this field to a somewhat lower sensitivity (rms $\simeq 0.5$ mJy) at an angular resolution of $45''$. In addition, we have examined images from the 92 cm Westerbork Northern Sky Survey (WENNS – Rengelink et al. 1997), the Greenbank 20 cm single-dish image (Condon & Broderick 1991), and the Greenbank 6 cm catalog (Becker, White, & Edwards 1991), as well as observing a portion of the field again at 6 cm on 12 January 1997 with the VLA in its D configuration.

Only one radio source in the EGRET error circle is coincident with an X-ray source: the single unidentified source RX J2229.0+6114. An image of this radio source constructed from the I , Q , and U maps of the NVSS is displayed in Figure 4a where it is seen that RX J2229.0+6114 lies at the center of an incomplete circular radio shell with a diameter of $3'.5$. The NVSS catalog lists two components for this source with a combined total flux density of $\approx 73 \pm 5$ mJy. More remarkable is the high degree of linear polarization present throughout the shell. The NVSS catalog lists a polarized flux density of ~ 21 mJy, albeit with large reported errors. However, we have constructed a polarization map from the archived Q and U data, and the signal is unmistakable. We find a peak polarized flux density of 3.9 mJy per beam (the map rms is 0.23 mJy) and an integrated polarized flux density of 17 mJy, yielding a polarized fraction of $\simeq 25\%$. In contrast, the 20 mJy source $4'$ south of the shell has a maximum polarized signal of 0.8 mJy, yielding an upper limit to its polarization of $\simeq 4\%$. Other sources in the field are also unpolarized at the 5% level. The polarization vectors are approximately radial throughout the shell, implying a tangential magnetic field. However, it is important to note that an unknown amount of Faraday rotation along the line of sight to the source could alter this interpretation.

Our additional observations of this source at 20 and 6 cm confirm its high degree of polarization. While our higher resolution data clearly over-resolve the source, leading to substantial missing flux density, both images also yield polarized fractions of $\simeq 30\%$; the 6 cm image is displayed in Figure 4b. The orientation of the polarization vectors at 6 cm are similar to those in the NVSS image, although they are not reliable since no polarization calibration was carried out during this observation. Note that the source $4'$ south of the shell is resolved in this map into an elongated structure $\approx 20''$ in extent, reminiscent of an extragalactic double radio source; its steep spectral index of $\alpha = 0.9$ (where $S_\nu \propto \nu^{-\alpha}$) derived from these data in conjunction with the WENNS catalog entry is consistent with this interpretation.

²The VLA, part of the National Radio Astronomy Observatory, is operated by Associated Universities, Inc., under cooperative agreement with the National Science Foundation.

No source is listed in the WENNS catalog at the position of radio shell. However, a map extracted from the archive shows a clear excess coincident with the shell; an image smoothed with a $60''$ Gaussian yields a crude estimated flux density of ~ 35 mJy, which is probably uncertain by a factor of 2. It is clear from this image, however, that while the southern source has peak and integrated flux densities of 51 mJy and 60 mJy, respectively, the shell source is not significantly brighter at 92 cm than it is at 20 cm.

The shell source is not detected in the Greenbank 20 cm images because of confusion with bright diffuse emission nearby, but is clearly seen in the Greenbank 6 cm maps; its flux density is listed in Becker et al. (1991) as 80 mJy. Since the $3.5''$ beam of the Greenbank telescope at this wavelength is well-matched to the source size, this is probably the most reliable measure of the source flux density, as all of the interferometric measurements resolve out some fraction of the flux. Our scaled-array observations with $\approx 15''$ beams yield the same flux densities at the two frequencies to within the relatively large errors. Thus, we conclude that all available measurements are consistent with a flat spectral index for the radio shell from 92 cm through 6 cm, with an integrated flux density of ≈ 80 mJy and a $\simeq 25\%$ polarized fraction.

There are no other notable radio sources in the error circle of 3EG J2227+6122. The brightest source, with a flux density at 6 cm of 494 mJy (Becker et al. 1991), is the H II region Sharpless 141. Most significant for the classification of the γ -ray source, however, is the fact that there is no compact, flat-spectrum radio source in this field comparable to the well-identified EGRET blazars, all of which have 6 cm flux densities in excess of 400 mJy (Mattox et al. 1997). The upper limit on such a source in the field of 3EG J2227+6122 is $\simeq 20$ mJy, the flux density limit of the Becker et al. catalog.

2.4. H α Imaging

To search for further evidence concerning the nature of the radio nebula and the compact X-ray source, we obtained H α images of an 7.3×7.3 region around VLA J2229.0+6114 using the MDM 2.4m telescope and a 39 \AA wide filter centered at 6563 \AA . Figure 5 shows the combined image. Diffuse H α structures are present throughout, with a peak surface brightness of $1.7 \times 10^{-16} \text{ erg cm}^{-2} \text{ s}^{-1} \text{ arcsec}^{-2}$ above the background level in the northwest and southeast corners of the image. This value is comparable to the average of the diffuse ionized gas at $b = 0^\circ$ near this location ($6.3 \times 10^{-17} \text{ erg cm}^{-2} \text{ s}^{-1} \text{ arcsec}^{-2}$; Reynolds 1985). However, there is no structure that appears correlated with either the radio shell or the location of the X-ray source. The 1σ noise level in this image is $1.2 \times 10^{-17} \text{ erg cm}^{-2} \text{ s}^{-1} \text{ arcsec}^{-2}$; the implications of the lack of H α emission at this level from VLA J2229.0+6114 or RX J2229.0+6114 will be discussed in §3.

2.5. *ASCA* Observation of the Unidentified Source RX J2229.0+6114

To investigate further the nature of RX J2229.0+6114, we obtained an *ASCA* observation beginning on 1999 August 4. A total of 114,500 s of exposure was obtained with each of the two GIS detectors, and 97,600 s with each of the two SIS detectors operated in 1-CCD mode. A prominent hard X-ray source was detected at the position (J2000) $22^h29^m05.^s9$, $+61^\circ14'16''$ (corrected for the *ASCA* temperature variation by the method of Gotthelf et al. 2000). This position is consistent with that of the *ROSAT* HRI source to within $8''$, and is well within the $12''$ radius *ASCA* error circle (at 90% confidence). A contour map of the combined *ASCA* GIS images is superposed on the *ROSAT* HRI images in Figure 1, and a more detailed view of the GIS image is shown in Figure 6. Analysis of the SIS and GIS photons from RX/AX J2229.0+6114, extracted using standard methods, shows that the spectrum (Figure 7) is best fitted by a power law of photon index $\Gamma = 1.51 \pm 0.14$ at 90% confidence, and $N_{\text{H}} = (6.3 \pm 1.3) \times 10^{21} \text{ cm}^{-2}$; the confidence contours of these spectral parameters are shown in Figure 8. The intrinsic 2–10 keV flux is $1.56 \times 10^{-12} \text{ erg cm}^{-2} \text{ s}^{-1}$.

Some care was required in the extraction of source and background regions for this analysis since there is also diffuse X-ray flux in this region. Weak, diffuse emission surrounding the compact source as well as to the northwest of it appears to be much softer than the compact source, and its uncertain distribution is a significant source of systematic error in the spectral parameters of RX/AX J2229.0+6114. We chose a radius of $4'$ for the source region in all detectors, and background regions which are as close as possible, but which exclude a region of radius $5'.25$ around the source. As we change the source and background extraction regions, the spectral index of RX/AX J2229.0+6114 can become as steep as 1.8, which we consider the maximum systematic deviation from the best fitted value of 1.51 ± 0.14 . There is also a weak, soft *ASCA* source coincident with the Herbig Ae/Be star RX J2226+6113. No other significant sources are seen in the *ASCA* images to a flux limit of $\sim 6 \times 10^{-14} \text{ erg cm}^{-2} \text{ s}^{-1}$.

The fitted $N_{\text{H}} = (6.3 \pm 1.3) \times 10^{21} \text{ cm}^{-2}$ of RX/AX J2229.0+6114 is almost equal to the total Galactic 21 cm column in this direction, $N_{\text{H}} = 8.4 \times 10^{21} \text{ cm}^{-2}$ (Stark et al. 1992), indicating that the X-ray source is at least 2 kpc distant, and possibly much farther. In the following sections we adopt a fiducial distance of 3 kpc as typical for the X-ray measured N_{H} if RX/AX J2229.0+6114 is Galactic. Absorption accounts for the relative weakness of the source in the HRI. The fitted *ASCA* spectral parameters would extrapolate to an HRI count rate of $(5.5 \pm 1.5) \times 10^{-3} \text{ counts s}^{-1}$, approximately twice that observed. This difference can be taken either as marginal evidence of long-term variability of this X-ray source, or as an indication that some extended emission is escaping detection by the HRI.

We also searched the *ASCA* spectrum of RX/AX J2229.0+6114 for an emission line of Fe $K\alpha$. No such line is detected, and 95% confidence upper limits on its EW range from 300 eV for a narrow line at $z = 0$, to 50 eV for a narrow line at $z = 0.12$. For a broad line (Gaussian $\sigma = 0.5 \text{ keV}$), the corresponding limits are 440 eV at $z = 0$ and 150 eV at $z = 0.12$. Beyond

$z = 0.12$, the X-ray luminosity of the source would exceed 10^{44} erg s $^{-1}$, and such luminous AGNs do not usually exhibit an Fe K α line.

The elapsed time of the *ASCA* observation was 67 h. During this time there was no evidence for short-term variability on time scales of hours. The *ASCA* GIS bit assignments were configured for high time resolution in order to search for pulsations. Approximately 54,600 s of data were obtained with 3.9 ms resolution, and 59,100 s with 0.5 ms resolution. These were searched, without success, for periodic pulsations for all periods as short as 10 ms using the Rayleigh test. In addition to a coherent search of the entire photon list (extracted from a region of radius 4' around RX/AX J2229.0+6114), the period search was performed on individual segments of 30,000 s in length in case there is a short-period pulsar with a large \dot{P} or acceleration. For example, the Crab pulsar's \dot{P} term contributes -0.17 cycles over an elapsed time of 30,000 s. Further searches of the data for a high B pulsar are in progress, and the results will be reported in a subsequent paper.

3. Possible Interpretations of RX/AX J2229.0+6114 and VLA J2229.0+6114

3.1. A Chance Coincidence?

We considered the hypothesis that RX/AX J2229.0+6114 is a chance superposition of a Galactic or extragalactic X-ray source unrelated to the radio shell VLA J2229.0+6114. The X-ray properties of RX/AX J2229.0+6114 are by themselves inconclusive as to its Galactic or extragalactic origin. Power-law fits to the *ASCA* spectrum require a column density slightly less than the maximum Galactic 21 cm value, which allows either a background AGN or a distant Galactic source. The power-law photon index $\Gamma = 1.5$ is harder than that of most radio-quiet QSOs, but is typical for a γ -ray pulsar (Wang et al. 1998). Although there is no prominent Fe K α emission line as would be expected from a low-redshift Seyfert galaxy, we cannot rule out that this is a luminous QSO for which Fe K α is generally not seen. The absence of variability on short and long time scales is also ambiguous, since AGNs are often but not always variable during an observation of this length. The spatial resolution and sensitivity of the *ASCA* SIS are not adequate to determine if RX/AX J2229.0+6114 is spatially extended, which if true, would be strong evidence of a Galactic pulsar-powered nebula. Similarly, it is not possible to conclude whether or not the diffuse soft X-ray emission surrounding RX/AX J2229.0+6114 is associated with it.

The absence of an emission-line optical counterpart to a limit of $R > 23$ somewhat favors a neutron star, although the Galactic absorption $A_R = 4.6$ mag (Schlegel et al. 1998) allows for the possibility that a faint object in the error circle in Figure 3 is a QSO of dereddened $R \approx 18.4$. Such a QSO would have $\alpha_{\text{ox}} \approx 1.0$, which would be near the extreme of X-ray loudness among QSOs (Wilkes et al. 1994). Thus, we regard the absence of a suitable optical counterpart for RX/AX J2229.0+6114 as somewhat discouraging an AGN classification unless it is a new type of extreme γ -ray quasar (see §4).

3.2. An H II Region?

We also considered the hypothesis that, if the X-ray source RX J2229.0+6114 is unrelated to the radio shell, then the latter might be an H II region. The principle reason for entertaining this possibility is the flat radio spectrum of VLA J2229.0+6114, which is reminiscent of thermal bremsstrahlung for which $S_\nu \propto \nu^{-0.1}$ in the radio. While the high degree of polarization strongly favors nonthermal emission, we also have independent evidence against the H II region hypothesis from our optical imaging. The argument proceeds as follows. We can use the observed radio flux to estimate the required electron density and ionizing flux. The thermal bremsstrahlung emissivity is

$$\epsilon_\nu = 6.8 \times 10^{-38} \frac{Z^2 n_e n_i}{T^{1/2}} e^{-h\nu/kT} g_{ff}(\nu, T) \text{ erg cm}^{-3} \text{ s}^{-1} \text{ Hz}^{-1}. \quad (1)$$

Assuming $T = 8,000$ K and an observing frequency $\nu = 4.86 \times 10^9$ Hz, the Gaunt factor $g_{ff} \approx 4.91$. Approximating the nebula as a sphere of ionized hydrogen of radius $r_s = \theta d/2$ where $\theta \approx 3'$ is its angular diameter, the flux density received at Earth is

$$S_\nu = 0.095 \left(\frac{d}{3 \text{ kpc}} \right) n_e^2 \text{ mJy}. \quad (2)$$

In this case, since we observe $S_\nu \approx 80$ mJy, the mean electron density in the nebula must be $n_e \approx 30 \text{ cm}^{-3}$.

The rate of ionizations Q is related to the Strömgen radius r_s and the case B recombination coefficient $\alpha_B(T) \approx 3.1 \times 10^{-13} \text{ cm}^3 \text{ s}^{-1}$ via

$$Q = \frac{4\pi}{3} r_s^3 n_e n_+ \alpha_B(T) = 8.4 \times 10^{43} \left(\frac{d}{3 \text{ kpc}} \right)^3 n_e^2 \text{ s}^{-1}. \quad (3)$$

Combining Equations (2) and (3), we can eliminate n_e and solve for Q as function of the observed radio flux and the unknown distance d ,

$$Q = 7.1 \times 10^{46} \left(\frac{d}{3 \text{ kpc}} \right)^2 \left(\frac{S_\nu}{80 \text{ mJy}} \right) \text{ s}^{-1}. \quad (4)$$

For a range of plausible distances between 2 and 8 kpc, Q is in the range $(0.32 - 5.0) \times 10^{47} \text{ s}^{-1}$, which corresponds to stars of spectral type B0. The absolute visual magnitudes of such stars are in the range -4.1 to -4.4 . Taking into account an estimated extinction $A_V = 1.4 \text{ mag kpc}^{-1}$ (up to a maximum of $A_V = 5.7$), the apparent magnitude of the exciting star should fall in the range $m_V = 10.3 - 15.8$.

The main difficulties with the H II region hypothesis are the absence of H α recombination radiation and the lack of a suitable exciting star. We describe each of these failed predictions in turn. Corresponding to the radio bremsstrahlung emission there should be H α with emission coefficient $\epsilon(\text{H}\alpha) = 3.2 \times 10^{-25} \text{ erg cm}^3 \text{ s}^{-1}$, giving a total observed flux of

$$F(\text{H}\alpha) = 8.2 \times 10^{-14} \left(\frac{d}{3 \text{ kpc}} \right) n_e^2 \text{ erg cm}^{-2} \text{ s}^{-1}. \quad (5)$$

It is more useful to relate the expected surface brightness in $H\alpha$ directly to the surface brightness in the radio image by combining Equations (2) and (5). Independent of any other variables, the proportionality is

$$\Phi(H\alpha) = 8.6 \times 10^{-16} \Sigma(4.86 \text{ GHz}), \quad (6)$$

where $\Phi(H\alpha)$ is the surface brightness of $H\alpha$ in $\text{erg cm}^{-2} \text{ s}^{-1} \text{ arcsec}^{-2}$ and $\Sigma(4.86 \text{ GHz})$ is the radio surface flux density in $\mu\text{Jy arcsec}^{-2}$. The peak observed $\Sigma(4.86 \text{ GHz})$ is $\approx 11 \mu\text{Jy arcsec}^{-2}$ in the northwest sector of the nebula, which predicts $\Phi(H\alpha) = 9.6 \times 10^{-15} \text{ erg cm}^{-2} \text{ s}^{-1} \text{ arcsec}^{-2}$. Even if we allow for the maximum extinction along the line of sight (4.6 mag at $H\alpha$), we would still expect to see a surface flux of $1.4 \times 10^{-16} \text{ erg cm}^{-2} \text{ s}^{-1} \text{ arcsec}^{-2}$ at this location, which should be a prominent feature in Figure 5. Instead, there is no sign of such emission to a limit at least one order of magnitude smaller. The absence of $H\alpha$ emission at this level is difficult to understand if the radio emission is truly thermal bremsstrahlung at $T \approx 8,000 \text{ K}$.

The second failing of the H II region hypothesis is the absence of an exciting star within the radio shell. The radio flux requires a B0 star of $10.3 \leq m_V \leq 15.8$. We have ruled out spectroscopically the bright star of $R \simeq 13$ at the bottom of Figure 3; it is an early K star. The A star of $R = 16.8$ closest to the X-ray source is also inadequate, as are half a dozen red stars of $R \approx 16 - 17$ which lie within the area of the radio shell. Thus, even after taking into account the maximum extinction along this line of sight, it is not likely that we have missed a star which could excite such an H II region at any distance less than 10 kpc. And at a larger distance than this, one would be suspicious of the presence of an H II region more than 500 pc from the Galactic plane. We consider that an H II region classification of VLA J2229.0+6114 is therefore ruled out by its high polarization and lack of corresponding optical evidence. Since we also lack an optical counterpart of RX/AX J2229.0+6114, we proceed to consider scenarios in which these sources could be Galactic objects associated with each other and powered by a neutron star.

3.3. A Young Supernova Remnant?

If VLA J2229.0+6114 and RX/AX J2229.0+6114 are associated, then it is highly likely that they reside in the Galaxy. We consider here whether the radio shell can be a small-diameter supernova remnant (SNR) or a pulsar wind nebula. The SNR hypothesis encounters an immediate difficulty, since shell components generally have steeper radio spectra characterized by $\alpha = 0.4 - 0.7$, where $S_\nu \propto \nu^{-\alpha}$. The compact cores of plerionic (Crab-like) remnants have flatter radio spectra ($\alpha = 0.0 - 0.3$), but they have center-filled morphologies.

The observed $\simeq 25\%$ linear polarization is high, but not unprecedented in Galactic SNRs. The integrated polarization of the Crab Nebula, for example, is $\sim 10\%$, but some features in the nebula show up to 50% linearly polarized flux (Wilson, Samarasinha, and Hogg 1985). The Crab-like remnant G21.5–0.9 exhibits 20–30% polarization in a circumferential ring, although the integrated polarized fraction for the whole remnant is somewhat lower (Becker & Szymkowiak

1981). The typical polarized fraction for shell-like remnants is 5–10%. Extragalactic radio sources also exhibit polarization, but typical values are a few percent, and no extended source with a polarized fraction $> 20\%$ at 20 cm has ever been detected. Irrespective of these comparisons, the high degree of linear polarization observed leads to the inescapable conclusion that the radio source associated with RX J2229.0+6114 is nonthermal.

There is no clear manifestation of the shell at any energy above the radio. The X-rays could be dominated by a point source, and our search for optical emission-line filaments, which was sensitive in the velocity range $\pm 1,000 \text{ km s}^{-1}$, yielded null results as described above. Nevertheless, it is clear that both the radio and the X-ray sources are nonthermal. The X-rays could be in part magnetospheric synchrotron emission from a young neutron star, and in part a compact plerion that is unresolved by the *ASCA* SIS. One way that a flat radio spectrum can be accommodated is if the characteristic synchrotron frequency of the lowest energy electrons is comparable to or greater than the observing frequency, with corresponding constraints on the magnetic field strength and electron energies as described in §3.4 below. $S_\nu \propto \nu^{+1/3}$ obtains in the low-frequency limit. Thus, there is enough evidence to warrant a SNR interpretation for VLA J2229.0+6114, albeit one with extreme properties.

3.4. A Pulsar Bow-Shock Nebula?

An alternative interpretation of the radio shell is nonthermal emission from a shock between a relativistic pulsar wind and the surrounding interstellar medium (ISM). Two scenarios can be considered for the required power in the pulsar wind. The first assumes that the shock is expanding with velocity v_s , and is driven by the difference in the interior and exterior pressure. The second method assumes that the radio shell is a bow shock which travels at the velocity of the pulsar v_p , and whose apex is located where the pulsar wind pressure equals $\rho_0 v_p^2$. Since the incomplete radio shell in fact resembles a bow shock, we chose the latter scenario for consideration. Thus, the spin-down power \dot{E} is related to the ambient ISM density $\rho_0 (\approx 1.4 n_H m_p)$ and the apex distance r_0 via

$$\dot{E} = 4\pi r_0^2 c \rho_0 v_p^2 = 1.9 \times 10^{38} \left(\frac{n_H}{0.1}\right) \left(\frac{d}{3 \text{ kpc}}\right)^2 \left(\frac{v_p}{100 \text{ km s}^{-1}}\right)^2 \text{ erg s}^{-1}. \quad (7)$$

Here we have measured 1.7 for the apex distance, and we assume a relatively low-density ISM. The rather large size of the radio shell means that the required \dot{E} is of order $10^{38} \text{ erg s}^{-1}$ for any reasonable distance, pulsar velocity, or ISM density.

It is worth noting that the direction of the pulsar’s velocity vector under this hypothesis is nearly perpendicular to and away from the Galactic plane, consistent with its birth as a young star in the disk. While not in itself strong evidence that this is a young pulsar, a velocity in the opposite direction would have been difficult to accommodate, as this source is already at just about the maximum z -height expected for a Population I object ($z = 160 \text{ pc}$ for $d = 3 \text{ kpc}$).

Under the bow shock hypothesis we assume that the radio flux is nonthermal emission from the shocked pulsar wind itself – i.e., the reverse shock rather than the shocked ISM – as theorized by Hester & Kulkarni (1988) in their model of the core of the supernova remnant CTB 80. A Crab-like pulsar wind is thought to contain relativistic electrons with $\gamma \approx 1 \times 10^6$ (Kennel & Coroniti 1984a,b). We hypothesize an electron-positron wind, and we suppose that the shock produces a relativistic Maxwellian distribution of particle energies rather than a power law, and an equipartition magnetic field of $B \approx 4 \times 10^{-5}$. Then the synchrotron power (in νF_ν) will be emitted mostly near $\nu \approx 25 \nu_c \approx 4 \times 10^{15}$ Hz (Tavani 1996) where ν_c is the characteristic frequency $\nu_c = (3\gamma^2 eB)/(4\pi m_e c)$. If a suprathermal power-law tail develops, then the frequency of the synchrotron peak can move down a factor of 10 to $\nu \approx 2.5 \nu_c \approx 4 \times 10^{14}$ Hz. Thus, we may expect little X-ray emission coincident with the radio shell. The low-energy limit of the synchrotron emission from such a thermal distribution has an asymptotic spectrum of the form $F_\nu \propto \nu^{+1/3}$, just as in the non-thermal case.

Assuming that the observed radio flux extrapolates with $\alpha \approx 0.0$ up to 10^{16} Hz, the total synchrotron power from the bow shock is $\approx 8.6 \times 10^{36}$ erg s $^{-1}$, which is a significant fraction of the \dot{E} inferred from the radius of the shell. We would not easily detect the optical synchrotron emission from the reverse shock because its surface brightness would be at most $\approx 11 \mu\text{Jy arcsec}^{-2}$ as it is in the radio, which corresponds to 21.1 mag arcsec $^{-2}$ in the R band, or 25.7 mag arcsec $^{-2}$ after correcting for the maximum extinction. Any steepening of the spectral index above the radio band would further decrease this optical estimate.

The majority of \dot{E} may go into accelerating and heating the shocked ISM. Although the forward shock from such pulsar winds is sometimes detected in H α , the low density of the ISM in this case, and the relative inefficiency of the non-radiative shock which is usually inferred, would predict much less H α emission than was required in the H II region scenario for VLA J2229.0+6114. A simple scaling relation can be derived to approximate the average surface brightness in H α of a nonradiative shock. According to Raymond (1991), it is the neutral fraction of hydrogen passing freely through the shock that emits on average 0.2 H α photons per atom via collisional excitation before it is ionized by the hot, shocked ISM. This number is relatively independent of shock velocity because the collisional excitation and collisional ionization cross sections scale similarly with temperature. If the bulk of the H α is emitted in a hemispherical region of radius r_0 , then the average H α surface brightness is

$$\Phi(\text{H}\alpha) = 1.1 \times 10^{-18} \left(\frac{n_{\text{H}}}{0.1} \right) \left(\frac{v_p}{100 \text{ km s}^{-1}} \right) \text{ erg cm}^{-2} \text{ s}^{-1} \text{ arcsec}^{-2}. \quad (8)$$

After including the effects of extinction, this value is 2–3 orders of magnitude smaller than the limiting sensitivity of our H α image.

In this scenario, neither the reverse shock nor the forward shock are energetic enough to emit the hard X-rays which are seen from RX/AX J2229.0+6114. Since the X-rays are apparently more compact in size than the radio shell, we would assume that they are entirely magnetospheric synchrotron emission from a young neutron star and/or a compact plerion that is unresolved by

the *ASCA* SIS. Its power-law spectral index $\Gamma = 1.5$ is compatible with this interpretation, as is its lack of variability. The 2–10 keV luminosity of this source is $1.7 \times 10^{33} (d/3 \text{ kpc})^2 \text{ erg s}^{-1}$, which is $\approx 10^{-5}$ of the pulsar spin-down power as inferred from the bow-shock interpretation of the radio shell. This is perhaps one of the weaknesses of this model, since the ratio L_x/\dot{E} for rotation-powered pulsars is typically observed to be $10^{-4} - 10^{-3}$. While \dot{E} can perhaps be reduced by lowering the ambient density n_{H} to 0.01, the unusual flat radio spectrum of VLA J2229.0+6114 remains a significant mystery. Thus, none of the scenarios that we have considered is without difficulty.

3.5. A Pulsar Wind Bubble?

Some of the problems associated with the large spin-down power inferred from the bow-shock interpretation of the radio source VLA J2229.0+6114 could be ameliorated if it is a bubble confined by the static pressure nkT of the ISM instead of the dynamic pressure $\rho_0 v_p^2$. This scenario would require the pulsar to have fortuitously a smaller velocity than the thermal speed of the ISM, but if it did, the inferred spin-down power could be much smaller,

$$\dot{E} = 4\pi r_0^2 c(n_e + n_i)kT = 2.4 \times 10^{36} \left(\frac{n_{\text{H}}}{0.1}\right) \left(\frac{d}{3 \text{ kpc}}\right)^2 \left(\frac{T}{10^4 \text{ K}}\right) \text{ erg s}^{-1}. \quad (9)$$

We assume an ambient temperature of $\sim 10^4$ K as appropriate if the ISM were pre-ionized by the recent UV flash from the supernova which produced the neutron star, or if an older pulsar is now surrounded by the cooling remnant of the past supernova shock. In this case, the X-ray luminosity could indeed be $10^{-4} - 10^{-3}$ of \dot{E} as is observed from most other pulsars. We would still not expect to detect diffuse optical continuum or H α emission associated with the radio shell, although the extrapolated radio spectrum of the shell would have to turn down below $\sim 10^{15}$ Hz in order not to exceed \dot{E} . The pulsar would then be required to have a very high efficiency of conversion of \dot{E} into γ -rays if it were to be the counterpart of the EGRET source 3EG J2227+6122. The observed photon flux of 3EG J2227+6122 above 100 MeV, $4.1 \times 10^{-7} \text{ photon cm}^{-2} \text{ s}^{-1}$ translates, for the photon spectral index of 2.14, into a luminosity of $3.7 \times 10^{35} (d/3 \text{ kpc})^2 \text{ erg s}^{-1}$, approximately 15% of \dot{E} from Equation (9). Such high γ -ray efficiencies are also inferred for the adolescent pulsars Geminga and PSR B1055–52; they could be reduced by a modest amount of anisotropy in the γ -ray beam pattern. It could be argued that the shape of the radio source VLA J2229.0+6114 resembles an incomplete spherical bubble as much as it does a cometary bow-shock surface.

4. Implications of the Identification (or Not) of 3EG J2227+6122

Despite the lack of a completely satisfactory theory linking the X-ray source RX/AX J2229.0+6114 and the radio shell VLA J2229.0+6114, we are encouraged that their properties are not inconsistent with what we would expect for a pulsar counterpart of

3EG J2227+6122. Of all the pulsars detected by EGRET, the Crab is the only one whose γ -ray spectral index ($\Gamma = 2.19 \pm 0.02$) is identical to that of 3EG J2227+6122 ($\Gamma = 2.24 \pm 0.14$). All of the less energetic pulsars have flatter spectra, and there is a clear trend of spectral flattening (and increasing γ -ray efficiency) with increasing age or decreasing spin-down power. Furthermore, since the observed γ -ray flux of the Crab is approximately 5 times that of 3EG J2227+6122, the estimated distance to RX/AX J2229.0+6114 of 3 kpc, 1.5 times that of the Crab, is basically what one would expect for a pulsar of half the spin-down power and similar γ -ray efficiency. At this intermediate Galactic latitude of 3° , a distance of 3 kpc is just about the maximum that one would expect for a young Population I object which should be found within the ISM layer of the disk, and it is just about right to accommodate the observed X-ray absorption column of $6.3 \times 10^{21} \text{ cm}^{-2}$. Essentially, by selecting an EGRET source at this Galactic latitude, we are predisposed to finding a pulsar that is similar to the Crab but more distant. Accordingly, it is perhaps not surprising that the bow-shock interpretation of the radio shell VLA J2229.0+6114 requires $\dot{E} \sim 2 \times 10^{38} \text{ erg s}^{-1}$, about half that of the Crab. If this identification for 3EG J2227+6122 is correct, the main difference between it and the Crab would be the presence of a prominent bow shock, and the relative weakness of X-ray emission from the pulsar magnetosphere and/or plerion. The failure to detect X-ray pulsations from RX/AX J2229.0+6114 is mysterious, however, unless a compact plerion dominates over the pulsar emission.

We presented an alternative scenario in which the spin-down power of the putative pulsar could be much lower, $\approx 2.4 \times 10^{36} \text{ erg s}^{-1}$. Although this would allow an older and therefore more “common” class of pulsar, the 3 kpc distance would strain its γ -ray production efficiency if it behaves similarly to γ -ray pulsars in this regime of \dot{E} , such as Vela, PSR B1951+32, and PSR B1706–44. Those three pulsars have (isotropic) γ -ray efficiencies between 0.4% and 7%, while a γ -ray luminosity of $3.7 \times 10^{35} (d/3 \text{ kpc})^2 \text{ erg s}^{-1}$ for 3EG J2227+6122 would require an efficiency of 15%. Perhaps this is not implausible, however, because the older pulsars Geminga and PSR B1055–52 have even higher apparent efficiency. Thus, it is possible that we are dealing with a highly efficient example of an intermediate age γ -ray pulsar.

The observed X-ray spectral index of RX/AX J2229.0+6114, $\Gamma = 1.5$, was in fact predicted for strong γ -ray pulsars by Wang et al. (1998) in the context of the outer-gap model. In this model, an outer-gap accelerator sends e^\pm pairs flowing inward and outward along open magnetic field lines. These particles continuously radiate γ -rays by the curvature mechanism. When the inward flowing particles approach the surface of the star, the $> 100 \text{ MeV}$ γ -rays that they emit convert into secondary e^\pm pairs in the inner magnetosphere wherever $B \sin\phi > 2 \times 10^{10} \text{ G}$, where ϕ is the angle between the photon and the \mathbf{B} field. Those secondary pairs must radiate away their energy instantaneously in the strong local \mathbf{B} field. Such a synchrotron decay spectrum has $\Gamma = 1.5$ between $E_{\min} = 0.1 \text{ keV}$ and $E_{\max} = 5 \text{ MeV}$. We emphasize that in this theory, the X-ray power-law is *not* supposed to be a simple continuation of the EGRET spectrum. Rather, it is a separate component radiated by the secondary e^\pm pairs that are created when some of the primary

γ -rays convert in the strong \mathbf{B} field. The X-ray luminosity generated by this mechanism is

$$L_x(2 - 10 \text{ keV}) \approx 1.5 \times 10^{31} f \left(\frac{0.1}{P}\right)^2 \left(\frac{B_p}{10^{12}}\right)^{1/2} \text{ erg s}^{-1}, \quad (10)$$

where P is the rotation period, B_p is the surface polar magnetic field, and f is the fraction of the Goldreich-Julian current that flows through the outer-gap accelerator back to the polar cap. This mechanism could make a significant contribution to the observed X-ray luminosity of RX/AX J2229.0+6114 only if P is small, ~ 0.01 s, *and* if f is of order unity. Otherwise, most of the X-rays must be generated by another mechanism, including perhaps an extended synchrotron nebula.

An alternative hypothesis, that RX/AX J2229.0+6114 is a twin of the intermediate-age pulsar Geminga, would be difficult to accommodate since Geminga's $\dot{E} = 3.3 \times 10^{34} \text{ erg s}^{-1}$ is inadequate to account for the γ -ray luminosity of 3EG J2227+6122 at a distance of 3 kpc unless a beaming factor > 10 is supposed. Also, the nonthermal X-ray luminosity of RX/AX J2229.0+6114, $1.7 \times 10^{33} (d/3 \text{ kpc})^2 \text{ erg s}^{-1}$, is 3 orders of magnitude more than that of Geminga.

If RX/AX J2229.0+6114 proves *not* to be the identification of 3EG J2227+6122, then the absence of any other X-ray candidate at the level of $\sim 4 \times 10^{-14} \text{ erg s}^{-1}$ is difficult to reconcile with any of the established classes of γ -ray emitters. If 3EG J2227+6122 is a pulsar but RX/AX J2229.0+6114 is *not* its counterpart, it implies that highly efficient (or highly beamed) γ -ray pulsars can avoid producing soft or hard X-rays at a level below 10^{-4} of their apparent γ -ray luminosity. At least two mechanisms of X-ray emission have been observed to accompany all γ -ray pulsars at such levels or higher, and they were explained in the context of the outer-gap model by Wang et al. (1998). One is the synchrotron emission from secondary pairs as described above. The second is thermal emission from the heated polar caps that are impacted by the inward-going accelerated particles from the outer-gap accelerator, as well as from the original heat of formation emitted over the whole surface. If 3EG J2227+6122 were a low-luminosity pulsar like Geminga, then it must be less than 1 kpc distant in order to be detected by EGRET, yet the intervening column density must be greater than 10^{21} cm^{-2} in order for its thermal soft X-rays not to reach us. Many of the unidentified EGRET sources could be similarly situated radio-quiet pulsars, made exceedingly difficult to identify in X-rays because of interstellar absorption.

One might still hypothesize that 3EG J2227+6122 is an extragalactic object. The one tempting piece of evidence along those lines is the steep γ -ray spectral index, which if it is not due to a Crab-like pulsar, is compatible with many of the known EGRET blazars. But as discussed above, there is no compact, flat-spectrum radio source in this field to an upper limit ≈ 20 mJy, or 50–100 times fainter than the typical identified EGRET blazars. Furthermore, there is no extragalactic X-ray source in this field other than possibly RX/AX J2229.0+6114 itself, and it is radio quiet (as a compact source) at the 1 mJy level. Thus, there is no escaping the fact that 3EG J2227+6122 would be a member of a new class of γ -ray source if extragalactic. However, it would not necessarily be unique in this regard. Similar considerations concerning the high-latitude source 3EG J1835+5918 were recently presented by Mirabal et al. (2000), where even more

stringent upper limits to its potential pulsar or blazar counterparts were obtained. Since many EGRET sources remain unidentified, more of them may prove, upon detailed study and especially after more precise localizations are obtained by *GLAST*, to be of a previously unrecognized type, for example, the frequently imagined “radio-quiet blazar”. It is of interest that several γ -ray loud quasars are seen to have flat X-ray spectra in the 2–10 keV band, with $\Gamma = 1.3 - 1.5$ (Tavecchio et al. 2000). Their broad-band spectra can be fitted with Inverse Compton jet models only if a significant proton component or Poynting flux outside the emission region is the main carrier of power. If RX/AX J2229.0+6114 were a radio-quiet blazar of this type, then its flat X-ray spectrum and lack of an optical counterpart might be just what is needed for the prototype of a new or extreme class of γ -ray loud AGN.

5. Conclusions

ROSAT and *ASCA* observations of the error circle of 3EG J2227+6122 reveal only one candidate X-ray counterpart with an intrinsic 2–10 keV flux of 1.56×10^{-12} erg cm $^{-2}$ s $^{-1}$, fitted by a power-law spectrum of photon index $\Gamma = 1.51 \pm 0.14$ and $N_{\text{H}} = (6.3 \pm 1.3) \times 10^{21}$ cm $^{-2}$. There is no other candidate to a flux limit of $\sim 6 \times 10^{-14}$ erg cm $^{-2}$ s $^{-1}$. This X-ray source happens to coincide with a highly polarized, incomplete radio shell which resembles a bow-shock nebula or a wind-blown bubble. The X-ray measured column density implies a distance of ≈ 3 kpc, although an extragalactic source has not been ruled out definitively. The flat radio spectrum is different from that of all other shell SNRs, and our optical searches have turned up no evidence for associated emission-line gas. On balance, we favor the hypothesis that RX/AX J2229.0+6114 is indeed an energetic pulsar counterpart of 3EG J2227+6122, and that VLA J2229.0+6114 is an associated nebula powered by a large fraction of the pulsar spin-down power. The best method for proving this and quantifying the age and energetics of this unique source would be to obtain more sensitive X-ray imaging and timing observations. We have planned both *Chandra* and *XMM* observations. *Chandra* has the ability to resolve a point source from the hypothesized compact synchrotron nebula, and to obtain a precise position for deeper optical follow-up. *XMM* with its high throughput may permit a pulsar discovery and a precise ephemeris to be developed, which could then lead to detection of pulses in the archival *ASCA* and EGRET data, and in future observations by *GLAST*. Deeper optical spectroscopy, and possibly infrared imaging, would constitute a more definitive test for an extragalactic counterpart of RX/AX J2229.0+6114 such as a Seyfert galaxy or a quasar. The absence of such a counterpart would itself be strong evidence that RX/AX J2229.0+6114 is a neutron star.

This work was supported by NASA grants NAG 5-3229 and NAG 5-7814. We thank R. H. Becker for obtaining an optical spectrum with the Keck telescope, and M. Eracleous for assistance with other spectroscopic observations at Kitt Peak. We also thank R. H. Becker for calling our attention to the important polarization information contained in the NVSS images.

REFERENCES

- Becker, R. H., & Szymkowiak, A. E. 1981, *ApJ*, 248, L23
- Becker, R. H., White, R. L., & Edwards, A. L. 1991, *ApJS*, 75, 1
- Bertsch, D. L., et al. 1992, *Nature*, 357, 305
- Brazier, K. T. S., Kanbach, G., Carramiñana, A., Guichard, J., & Merck, M. 1996, *MNRAS*, 281, 1033
- Brazier, K. T. S., Reimer, O., Kanbach, G., Carramiñana, A. 1998, *MNRAS*, 295, 819
- Condon, J. J., & Broderick, J. J. 1991, *AJ*, 91, 1051
- Condon, J. J., Cotton, W. D., Greisen, E. W., Yin, Q. F., Perley, R. A., Taylor, G. B., & Broderick, J. J. 1998, *AJ*, 115, 1693
- Cusumano, G., Maccarone, M. C., Nicastro, L., Sacco, B., & Kaaret, P. 2000, *A&A*, 528, L25
- Frail, D. A., & Moffett, D. A. 1993, *ApJ*, 408, 637
- Gotthelf, E. V., Ueda, Y., Fujimoto, R., Kii, T., & Yamaoka, K. 2000, *ApJ*, 544, 000
- Halpern, J. P., & Holt, S. S. 1992, *Nature*, 357, 222
- Halpern, J. P., & Ruderman 1993, *ApJ*, 415, 286
- Hang, H.-R., Liu, Q.-Z., & Xia, J.-P. 1999, *A&A* 344, 614
- Hartman, R. C. et al. 1999, *ApJS*, 123, 79
- Helfand, D. J. 1994, *MNRAS*, 267, 490
- Hester, J. J., & Kulkarni, S. R. 1988, *ApJ*, 331, L121
- Kaaret, P., & Cottam, J. 1996, *ApJ*, 462, L1
- Kaaret, P., Piraino, S., Halpern, J., & Eracleous, M. 1999, *ApJ*, 523, 197
- Kaspi, V. M., Lackey, J. R., Mattox, J., Manchester, R.N., Bailes, M., & Pace, R. 2000, *ApJ*, 528, 445
- Kennel, C. F., & Coroniti, F. V. 1984a, *ApJ*, 283, 710
- . 1984b, *ApJ*, 283, 731
- Kuiper, L., Hermsen, W., Verbunt, F., Thompson, D. J., Stairs, L. H., Lyne, A. G., Strickman, M. S., & Cusumano, G. 2000, *A&A*, in press
- Lamb, R. C., & Macomb, D. J. 1997, *ApJ*, 488, 872
- Mattox, J. R., Schachter, J., Molnar, L., Hartman, R. C., & Patnaik, A.R. 1997, *ApJ*, 481, 95
- McLaughlin, M. A., Mattox, J. R., Cordes, J. M., & Thompson, D. J. 1996, *ApJ*, 473, 763
- Mirabal, N., Halpern, J. P., Eracleous, M., & Becker, R. H. 2000, *ApJ*, in press
- Monet, D., et al. 1996, USNO-SA2.0, (U.S. Naval Observatory, Washington DC)

- Oka, T., Kawai, N., Naito, T., Horiuchi, T., Namiki, M., Saito, Y., Romani, R. W., & Kifune, T. 1999, *ApJ*, 526, 764
- Radhakrishnan, V., & Cooke, D. J. 1969, *Ap Lett*, 3, 225
- Ramanamurthy, P. V., et al. 1995, *ApJ*, 447, L109
- Raymond, J. C. 1991, *PASP*, 103, 781
- Rengelink, R. B., Tang, Y., de Bruyn, A. G., Miley, G. K., Bremer, M. N., Röttgering, H. J. A., & Bremer, M. A. R. 1997, *A&AS*, 124, 259
- Reynolds, R. J. 1985, *ApJ*, 294, 256
- Roberts, M. S. E., & Romani, R. W. 1998, *ApJ*, 496, 827
- Roberts, M. S. E., Romani, R. W., Johnston, S., & Green, A. J. 1999, *ApJ*, 515, 712
- Romani, R. W. & Yadigaroglu, I.-A. 1995, *ApJ*, 438, 314
- Schlegel, D. J., Finkbeiner, D. P. , & Davis, M. 1998, *ApJ*, 500, 525
- Stark, A. A., Gammie, C. F., Wilson, R. W., Bally, J., Linke, R. A., Heiles, C., & Hurwitz, M. 1992, *ApJS*, 79, 77
- Strickman, M. S., et al. 1998, *ApJ*, 497, 419
- Tauris, T. M., & Manchester, R. N. 1998, *MNRAS*, 298, 625
- Tavani, M. 1996 *ApJ*, 466, 778
- Tavecchio, F. et al. 2000, *ApJ*, in press
- Vestrand, W. T., Sreekumar, P., & Mori, M. 1997, *ApJ*, 483, L49
- Wang, F. Y.-H., Ruderman, M., Halpern, J. P., & Zhu, T. 1998, *ApJ*, 498, 373
- Wilkes, B. J., Tananbaum, H., Worrall, D. M., Avni, Y., Oey, M. S., & Flanagan, J. 1994, *ApJS*, 92, 52
- Wilson, A. S., Samarasinha, N. H., & Hogg, D. E. 1985, *ApJ*, 294, L121
- Yadigaroglu, I.-A., & Romani, R. W. 1995, *ApJ*, 449, 211
- . 1997, *ApJ*, 476, 347
- Zinnecker, H., & Preibisch, Th. 1994, *A&A*, 292, 152

Table 1. *ROSAT* HRI X-ray Sources in the Field of 3EG J2227+6122

X-ray			Position		Unc. ^a	Counts	Optical		Position		<i>R</i>	<i>B</i>	ID			
R.A.		Decl.	R.A.				Decl.	<i>R</i>	<i>B</i>							
(h	m	s)	(°	'	"	(μ)	(ksec ⁻¹)	(h	m	s)	(°	'	"	(mag)	(mag)	
22	24	30.25	+61	28	19.0	±2.0	2.6 ± 0.9	22	24	30.39	+61	28	19.3	14.9	17.0	dMe star
22	26	28.26	+61	45	57.8	±2.4	1.6 ± 0.6	22	26	28.30	+61	45	55.5	14.3	16.0	M star
22	26	38.93	+61	13	30.2	±3.8	1.6 ± 0.6	22	26	38.79	+61	13	31.4	13.2	14.8	Herbig Ae/Be
22	29	04.97	+61	14	12.9	±2.7	2.5 ± 0.6	—————	—————	—————	≥ 21.3	> 24.0	—————			
22	29	29.09	+61	04	53.6	±1.4	2.3 ± 0.5	22	29	29.23	+61	04	52.2	12.9	13.9	K star
22	30	49.68	+61	30	52.5	±1.1	13.1 ± 1.2	22	30	49.32	+61	30	51.9	12.8	13.9	K star

^a 90% confidence uncertainty in each coordinate.

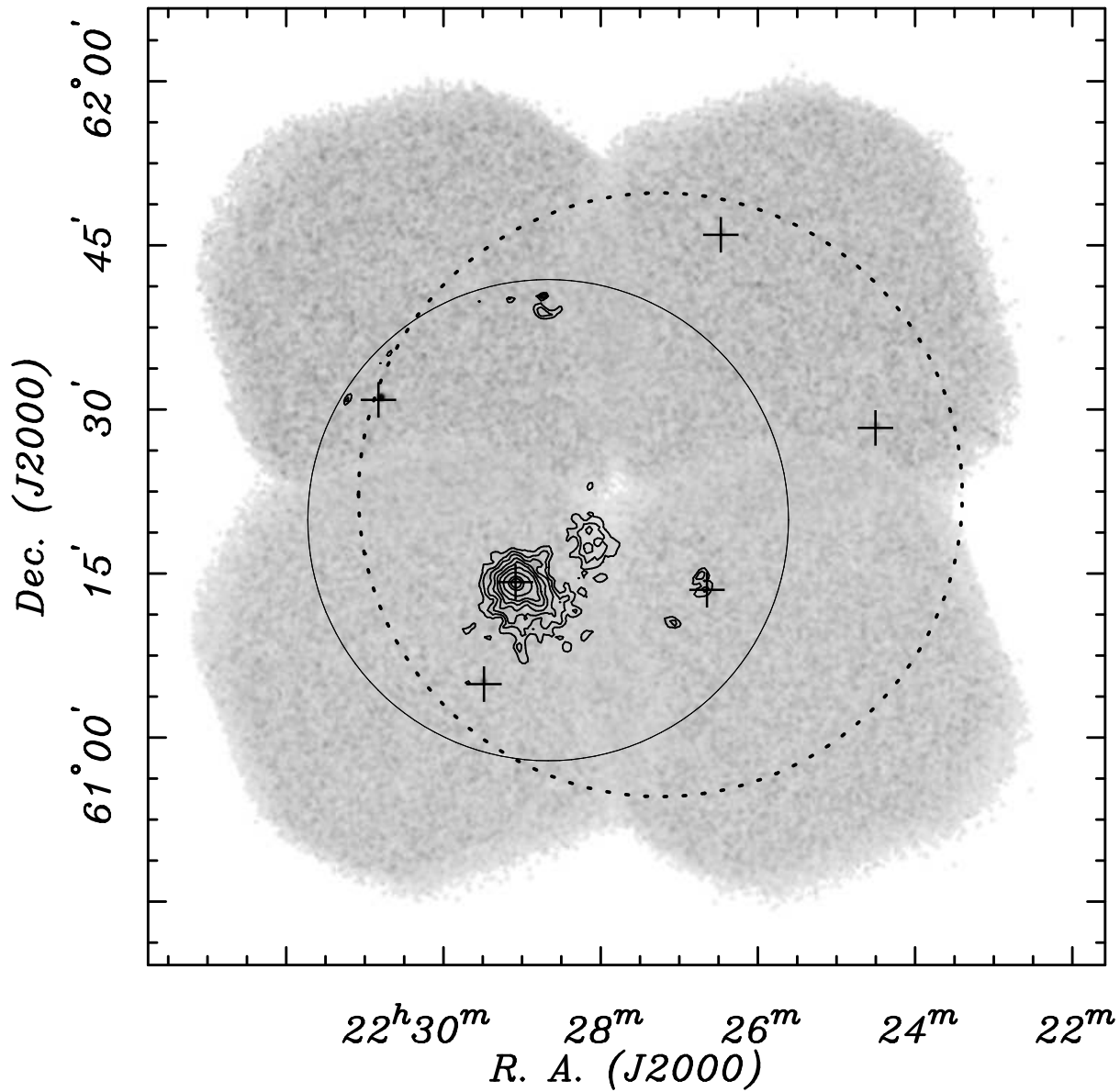


Fig. 1.— A montage of four *ROSAT* HRI images covering the 95% error circle of 3EG J2227+6122 (*dashed circle*). There are six *plus signs* at the locations of HRI sources (also listed in Table 1); all but one of these are bright stars. The *solid circle* and the contours within it are the *ASCA* GIS images, showing a bright, hard source coincident with the only unidentified HRI source.

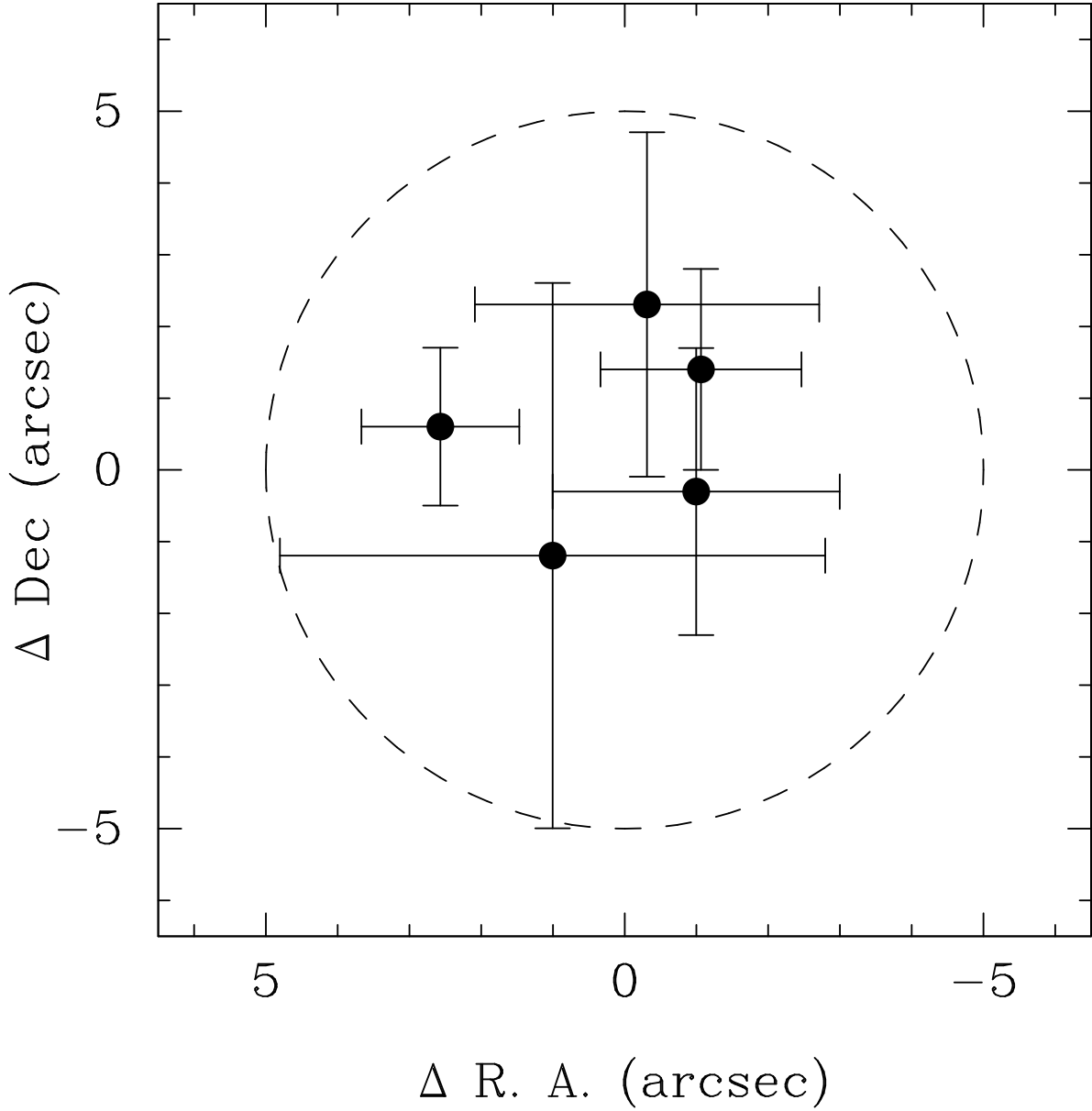


Fig. 2.— *ROSAT* HRI X-ray source positions and their 90% confidence uncertainties compared with the optical positions of the five bright stars with which they are identified. The offset between the X-ray and optical position is plotted. The illustrated 5'' radius circle is, therefore, a conservative error estimate on the position of the unidentified source RX/AX J2229.0+6114.

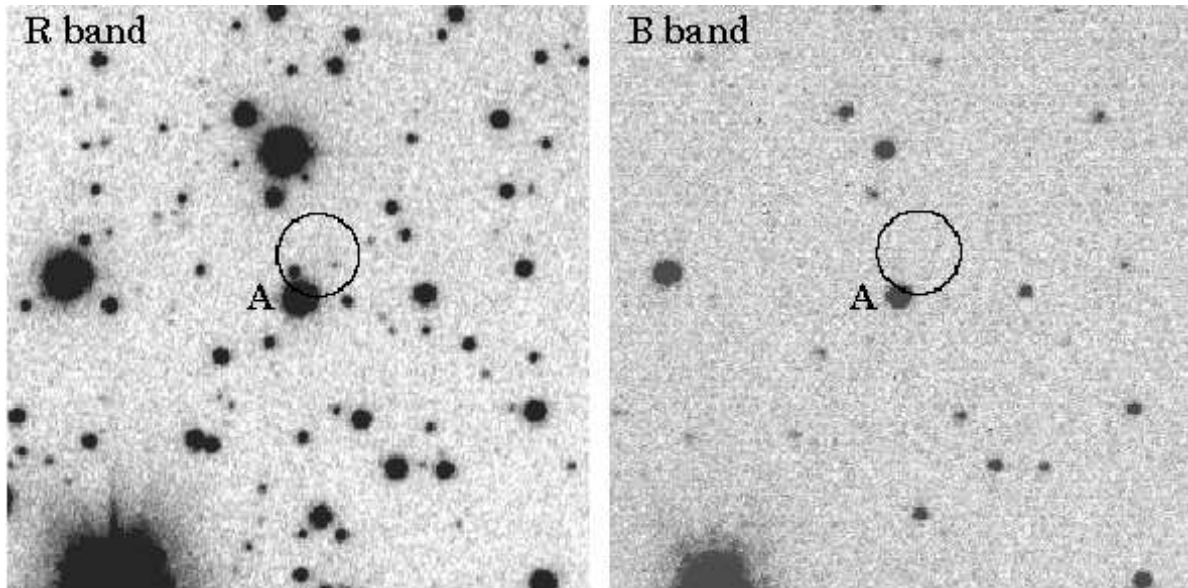


Fig. 3.— Optical images of the location of the unidentified X-ray source RX J2229.0+6114 from the MDM 2.4m telescope. The error circle is $5''$ in radius. Limiting magnitudes are 24.5 in R and 24.0 in B . Star A is a highly reddened A star, and the $R = 21.3$ object just north of it is either a star or a galaxy with no emission lines. The faintest detected object within the error circle has $R = 23.00 \pm 0.10$.

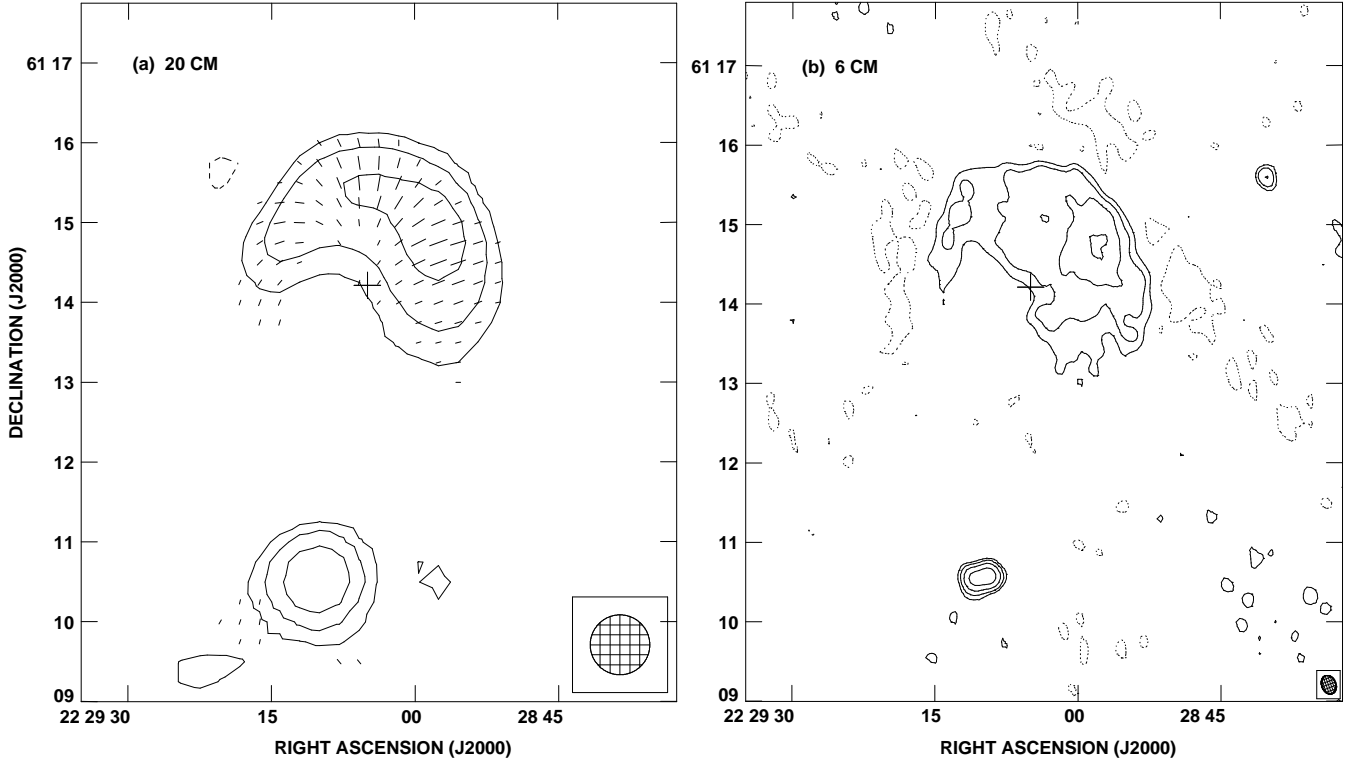


Fig. 4.— (a) The 20 cm NVSS map showing the shell-like radio source VLA J2229.0+6114 with polarization vectors superposed. The *plus sign* is the location of the X-ray source RX J2229.0+6114. Contour levels are 2.2, 4.4, and 8.8 mJy beam⁻¹. The length of the polarization vector corresponds to 0.30 mJy beam⁻¹ arcsec⁻¹. The hatched circle at the lower right represents the beam size. (b) A 6 cm VLA map obtained in the D configuration. The beam is a factor of 3 smaller than in a. Contour levels are -0.15, 0.15, 0.3, 0.6, and 1.2 mJy beam⁻¹. The resolved radio source below the shell has a steep spectrum and is presumably a background AGN. This background radio source is not detected in X-rays.

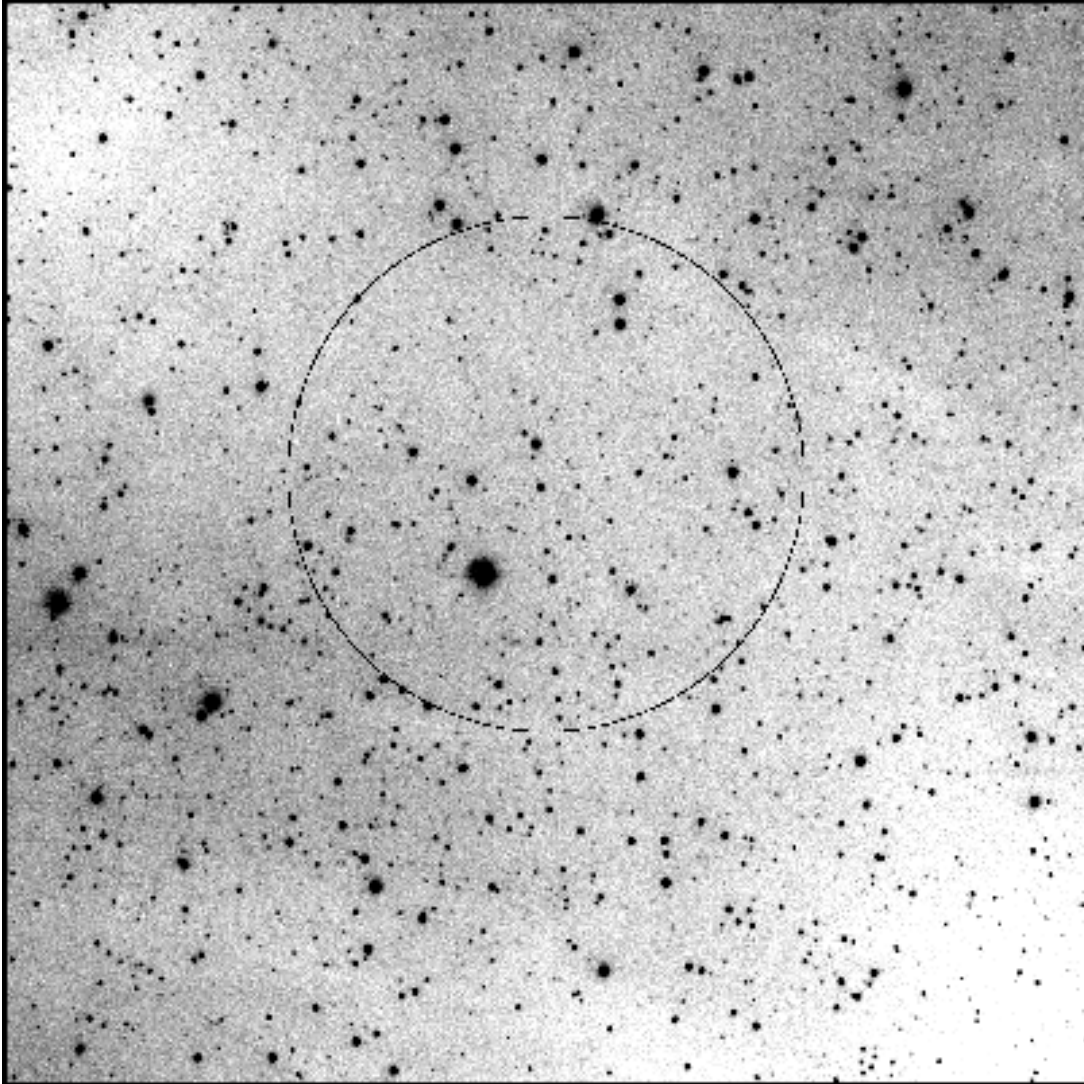


Fig. 5.— An $H\alpha$ image from the MDM 2.4m telescope of a $7'.3 \times 7'.3$ region around the radio shell VLA J2229.0+6114. A 39 \AA wide filter was used, and the brightest regions have a surface brightness of $1.7 \times 10^{-16} \text{ erg cm}^{-2} \text{ s}^{-1} \text{ arcsec}^{-2}$. The circle marks the approximate boundary of the radio shell as seen in Figure 4. There is apparently no $H\alpha$ emission associated with it.

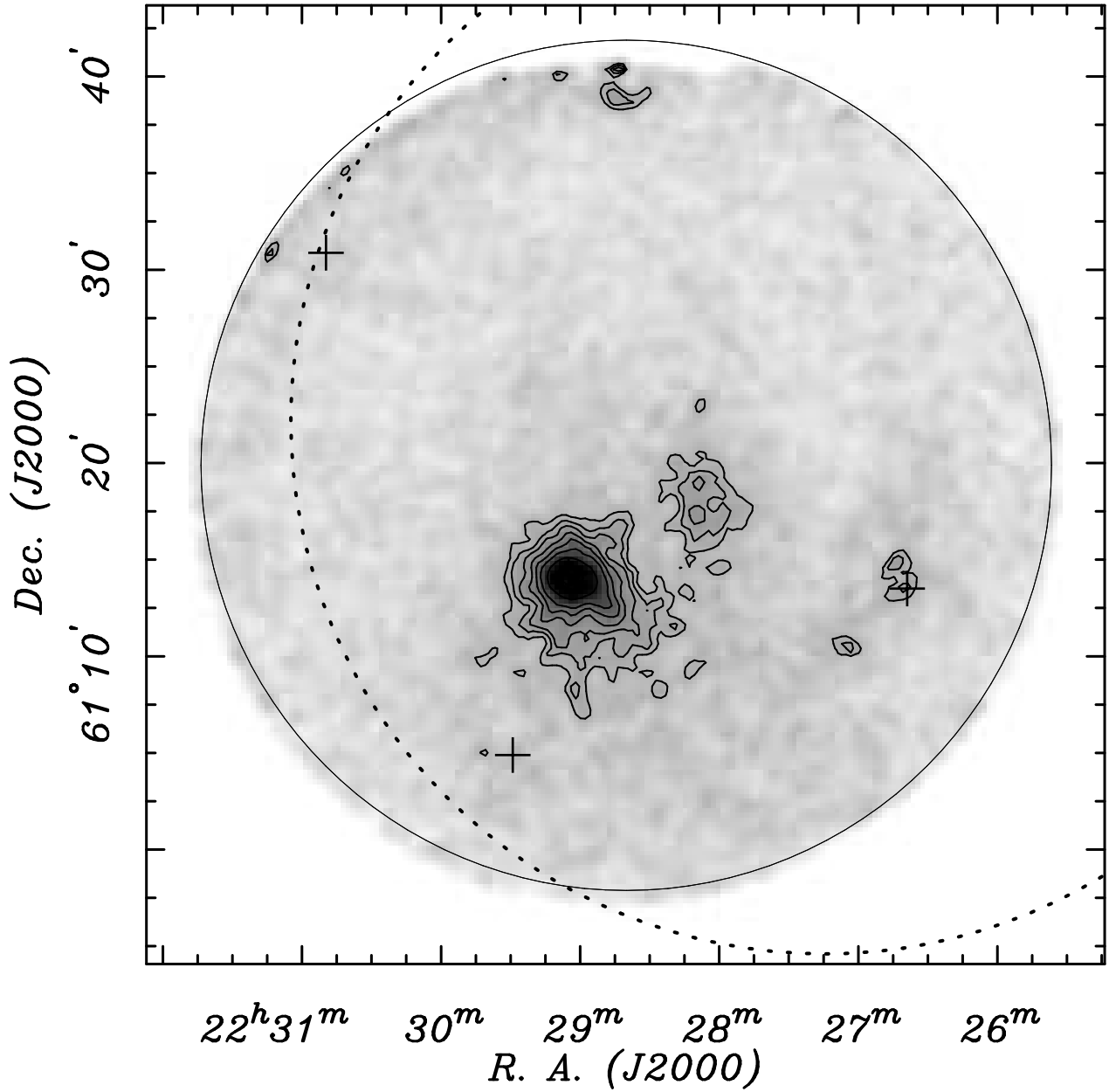


Fig. 6.— The *ASCA* GIS images in the 0.8–8.0 keV band, with the locations of *ROSAT* HRI sources (*plus signs*) superposed. Contours are used to highlight the grey scale. Diffuse, softer X-ray emission is evident surrounding the hard source RX/AX J2229.0+6114 and to the northwest of it. The weak source far to the west is coincident with the Herbig Ae/Be star.

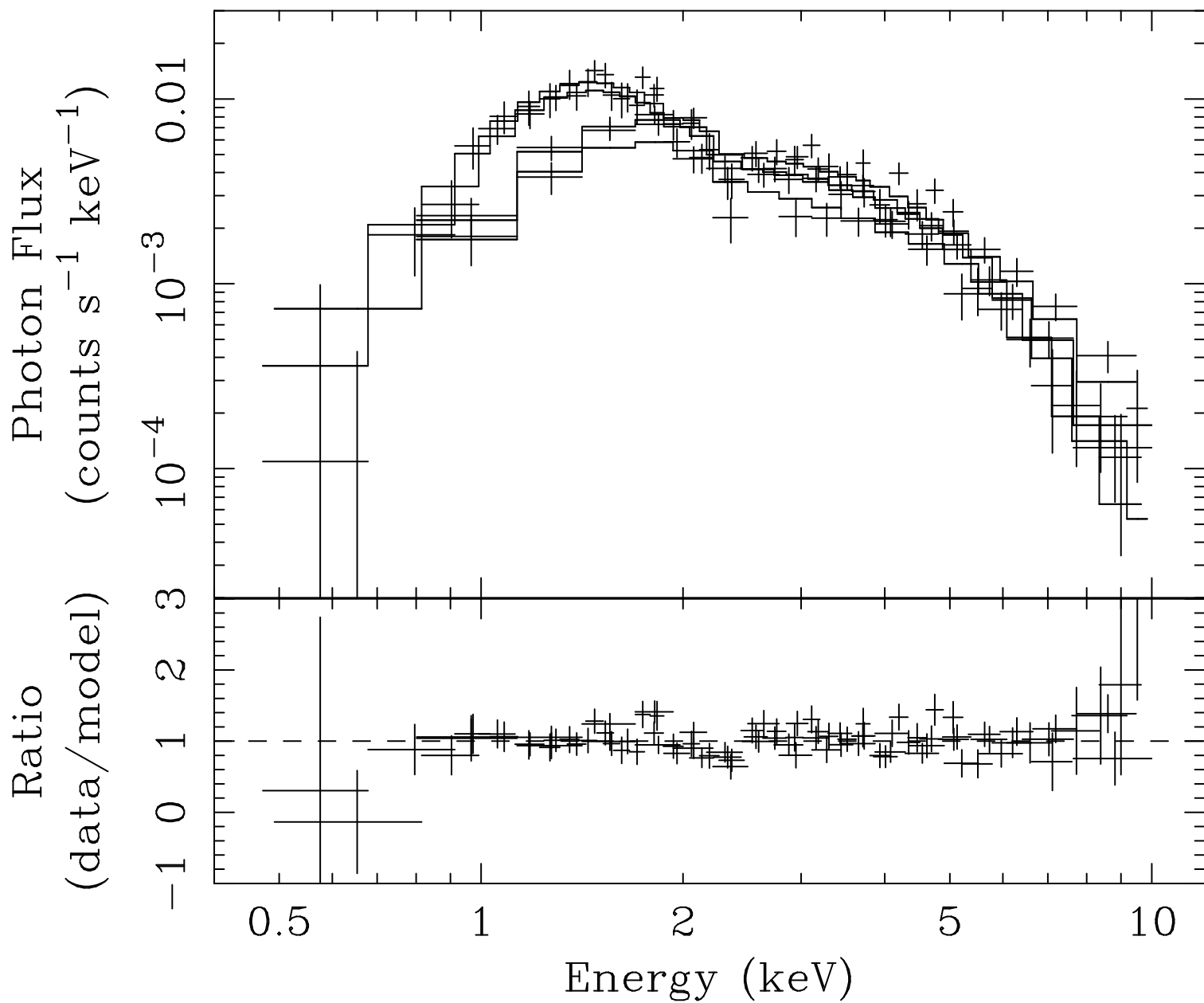


Fig. 7.— *ASCA* SIS and GIS spectra of RX J2229.0+6114, and residuals from a power-law fit.

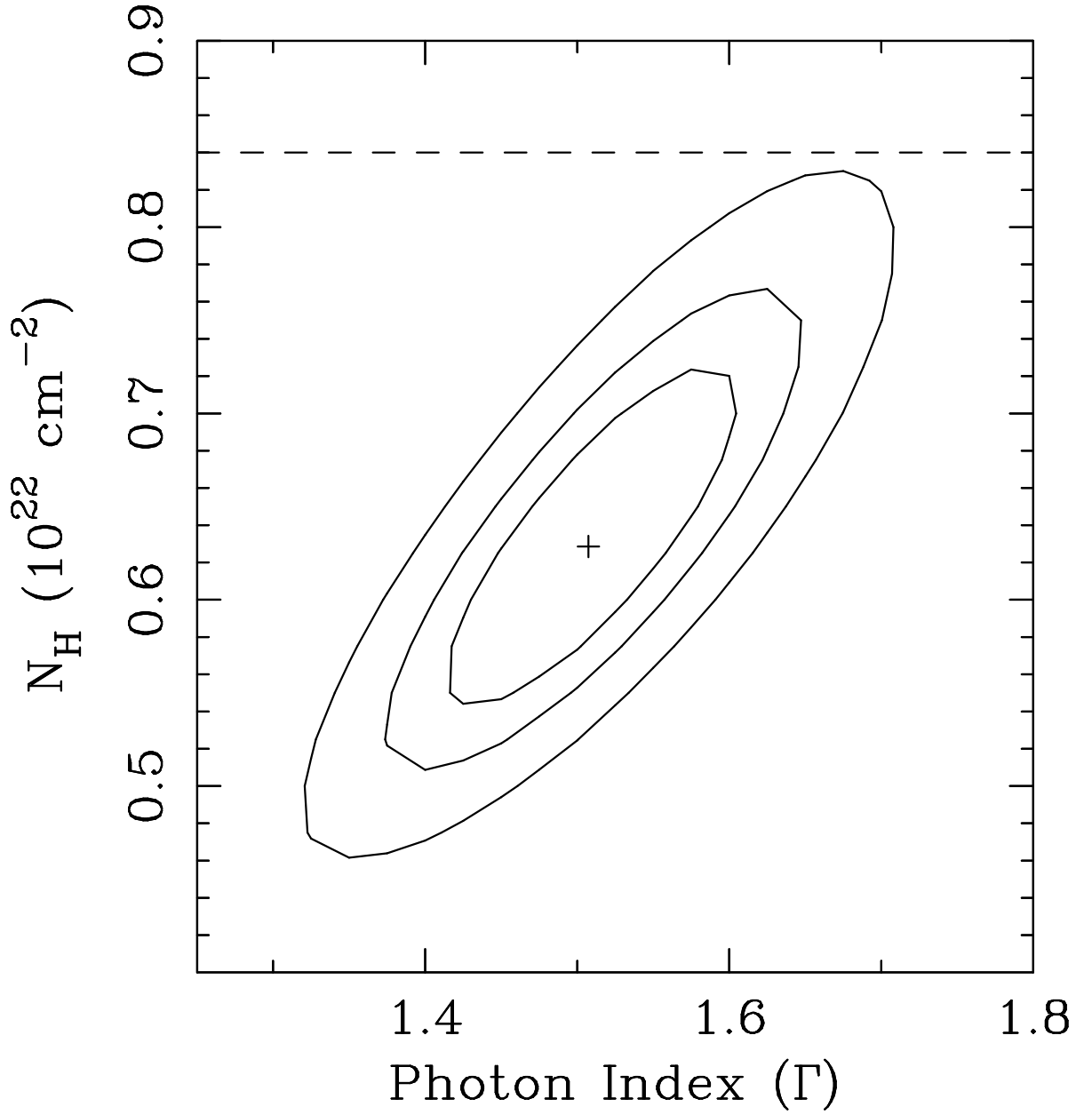


Fig. 8.— Confidence contours of parameters fitted to the *ASCA* spectrum of RX/AX J2229.0+6114. Confidence limits are 68%, 90%, and 99% for two interesting parameters. The total Galactic 21 cm column density in this direction is indicated by a dashed line.